HNPS Advances in Nuclear Physics

33rd Symposium of the Hellenic Nuclear Physics Society

Hellenic Nuclear Physics Society

HNPS Advances in Nuclear Physics

Editors:

T.J. Mertzimekis
P. Koseoglou

Proceedings of the 33rd Hellenic Symposium on Nuclear Physics and Applications

HNPS2025

National and Kapodistrian University of Athens

5 & 6 June 2025

Multinucleon Transfer Mechanisms in peripheral collisions of 40Ar + 64Ni at 15 MeV/nucleon.

Konstantinos Gkatzogias, Georgios Souliotis, Chrysi Giannitsa, Stergios Koulouris, Martin Veselsky, Sherry Yennello, Aldo Bonasera

doi: 10.12681/hnpsanp.8887

To cite this article:

ARTICLE

Multinucleon Transfer Mechanisms in peripheral collisions of ^{40}Ar + ^{64}Ni at 15 MeV/nucleon.

K. Gkatzogias,[*,1] G.A. Souliotis,[1] Ch. Giannitsa,[1] S. Koulouris,[1] M. Veselsky,[2] S.J. Yennello,[3] and A. Bonasera[3]

[1]Laboratory of Physical Chemistry, Department of Chemistry, National and Kapodistrian University of Athens, Athens, Greece

[2]Institute of Experimental and Applied Physics, Czech Technical University, Prague, Czech Republic

[3]Cyclotron Institute, Texas A&M University, College Station, Texas, USA

[*]Corresponding author: gkakonst@chem.uoa.gr

Abstract

We report a systematic study of ejectiles from the interaction of a 15 MeV/nucleon ^{40}Ar beam with a ^{64}Ni target. The experimental data were obtained with the MARS spectrometer at the Cyclotron Institute of Texas A&M University in previous work of our group. Theoretical calculations were performed with the Deep-Inelastic Transfer (DIT) and the Constrained Molecular Dynamics (CoMD) models, both coupled to the statistical decay code GEMINI. The resulting mass, angular and momentum distributions have been compared with the corresponding experimental distributions. Both models describe the general trends of the data in a satisfactory way. We plan to further explore the role of specific model parameters (nuclear potentials in DIT, nuclear compressibilities in CoMD) to provide further insight into the mechanisms of nuclear reactions below the Fermi energy (10–35 MeV/nucleon).

1. Introduction

The production of neutron-rich nuclides in peripheral heavy-ion collisions at Fermi energies (10–35 MeV/nucleon) remains an area of considerable interest in nuclear physics. Such systems allow access to nuclei far from the valley of β-stability, enabling detailed studies of the effective nuclear interaction and astrophysical processes, including the rapid neutron-capture process (r-process). In this energy regime, multinucleon transfer and deep-inelastic reactions occurring near and above the Coulomb barrier play a prominent role, leading to the formation of exotic neutron-rich projectile-like fragments. These reaction mechanisms, largely governed by sequential nucleon exchange, offer a valuable framework for exploring both nuclear structure and reaction dynamics [1–4].

In this work, we build upon our group's earlier studies of the ^{40}Ar + ^{64}Ni reaction at a beam energy

of 15 MeV/nucleon [5, 6]. The experimental data discussed here were previously collected using the Momentum Achromat Recoil Separator (MARS) at the Cyclotron Institute of Texas A&M University. To interpret the results, we employ two dynamical reaction models: the Deep-Inelastic Transfer (DIT) model [7] and the Constrained Molecular Dynamics (CoMD) model [8]. In both approaches, the subsequent de-excitation of primary fragments is simulated using the GEMINI code [9]. In this manuscript we are presenting the continuation of our previous studies, comparing model predictions with experimental observations via the systematic study of mass and momentum distributions. Additionally, preliminary results of the effect of the symmetry potential in the reaction dynamics are reported. [10–13].

2. Experimental Setup

The experimental data for the ^{40}Ar + ^{64}Ni reaction were collected using the MARS Separator at the Cyclotron Institute, Texas A&M University [14]. A ^{40}Ar^{9+} beam from the K500 Superconducting Cyclotron, accelerated to 15 MeV per nucleon, bombarded a ^{64}Ni target of 2 mg/cm^2 thickness. The target was positioned at an angle of 4.0° relative to the optical axis of MARS, allowing the detection of reaction ejectiles within the angular range 2.2°–5.8°, corresponding to a solid angle acceptance of $\Delta\Omega$ = 4 msr. Projectile fragments were first detected by a parallel-plate avalanche counter (PPAC) located at the dispersive image of MARS, which provided measurements of their position, magnetic rigidity, and START time. The ions were then focused to the end of the separator, where they passed through a second PPAC (providing STOP-time information) before being collected in a ΔE–E silicon detector telescope. The scanned magnetic rigidity range of 1.1–1.5 Tm did not encompass all reaction products, as shown in Fig. 1. This limitation reflects the intrinsic selectivity of spectrometer-based experiments, which are set to specific magnetic rigidity regions corresponding to the reaction products of interest. In the present case, the acceptance mainly covers projectile-like and neutron-rich fragments, while lighter products fall outside the scanned range. The same angular and magnetic rigidity constraints were applied to the theoretical calculations, allowing for a direct and meaningful comparison between experimental data and model predictions. The identification of projectile-like fragments was achieved on an event-by-event basis using standard techniques that combine measurements of magnetic rigidity, energy loss, residual energy, and time of flight, following the procedure described in [2].

3. Computational Models

The calculations were carried out using a two-step Monte Carlo approach. In the first step, the dynamical stage of the reaction is simulated using two theoretical models, described briefly below.

The Deep-Inelastic Transfer (DIT) model [7] is a phenomenological model designed to describe peripheral collisions in the Fermi energy domain. In this model, both the projectile and target nuclei are treated as spherical objects that follow Coulomb trajectories until they come within the range of the nuclear interaction. At that point, a stochastic exchange of nucleons occurs through a "window" formed at the contact region between the two nuclear surfaces.

The Constrained Molecular Dynamics (CoMD) model [8] provides a microscopic description of heavy-ion reactions. Based on the quantum molecular dynamics (QMD) formalism, it represents nucleons as localized Gaussian wavepackets in phase space that interact via an effective Skyrme-type potential. In our calculations, we use a standard value of the symmetry potential proportional to the density ($V_{sym}(\rho) \propto \rho$). We have also tested two additional options, a stiff ($V_{sym}(\rho) \propto \rho^2$) and a soft ($V_{sym}(\rho) \propto \sqrt{\rho}$) symmetry potential. [15]. Within the CoMD framework, the isovector part of the effective interaction is governed by the symmetry potential, whose density dependence reflects the underlying behavior of the nuclear symmetry energy. This term plays a key role in isospin trans-
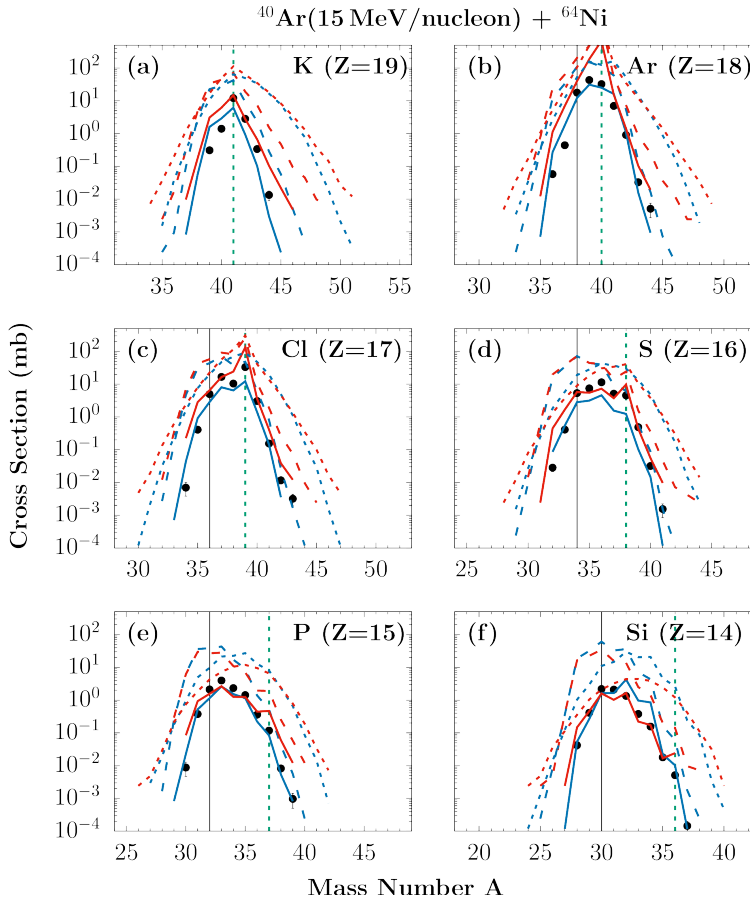
Figure 1. Production cross sections (mass distributions) of elements with Z = 14–19 from the reaction ^{40}Ar (15 MeV/nucleon) + ^{64}Ni. Black points: experimental data. (a)–(f): DIT/CoMD calculations (Blue/Red): Dotted lines: primary fragments, Dashed lines: final (cold) fragments, Full lines: final fragments filtered for angular acceptance and magnetic rigidity. The vertical dashed (green) lines indicate the initiation of neutron pickup. On the left of the vertical black lines the data are obtained with incomplete magnetic rigidity coverage.

port, nucleon exchange, and the evolution toward N/Z equilibration in heavy-ion collisions near the Fermi energy. Different symmetry potential parametrizations, commonly referred to as stiff and soft, correspond to different density dependences of the symmetry potential and are therefore expected to influence the production and kinematic properties of neutron-rich reaction products. [16] Recent studies by our group [6, 13] indicate that both the DIT and CoMD models can adequately describe the nucleon exchange mechanism as a sequential transfer of nucleons.

4. Results and Discussion

In this section, we present a comparison between our theoretical calculations and the experimental data. We also examine the sensitivity of the CoMD model to variations in its input parameters, particularly by comparing results obtained with the standard symmetry potential and with modified, stiffer and softer symmetry potentials. All the data correspond to the measured ejectiles from the reaction, as determined by the experimental setup described earlier.

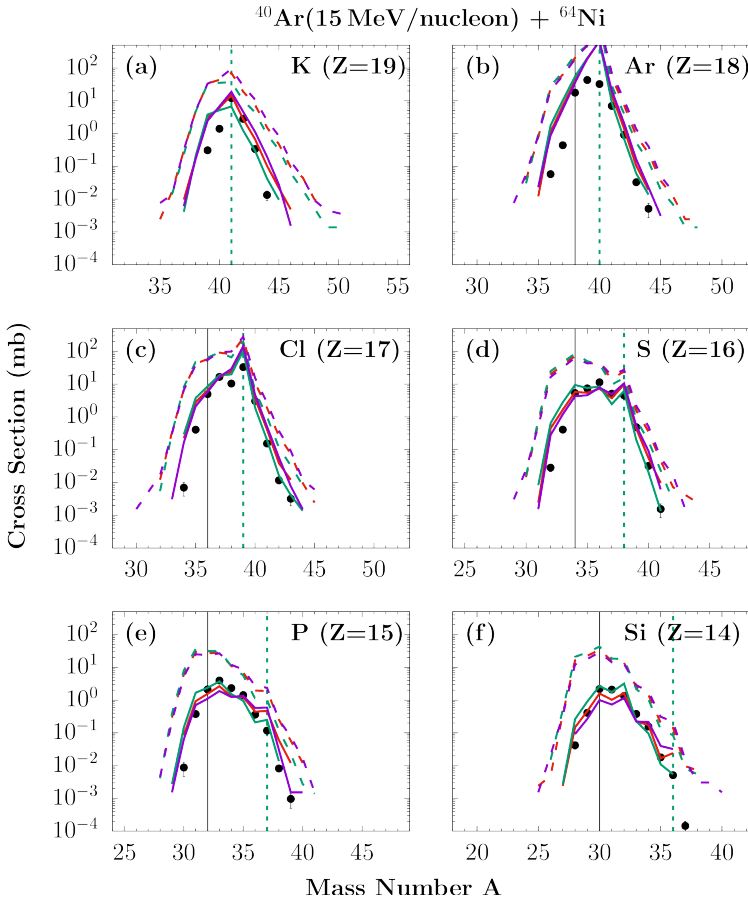Fig. 1 displays the isotope yields for elements with atomic numbers Z = 14 − 19. The experimental

$$^{40}\text{Ar}(15\,\text{MeV/nucleon}) + {}^{64}\text{Ni}$$

Figure 2. Production cross sections (mass distributions) of elements with Z = 14–19 from the reaction ^{40}Ar (15 MeV/nucleon) + ^{64}Ni. Black points: experimental data. (a)–(f): CoMD calculations with Standard/Stiff/Soft symmetry potential; (Red/Green/Purple): Dashed lines: final (cold) fragments, Full lines: final fragments filtered for angular acceptance and magnetic rigidity. The vertical dashed (green) lines indicate the initiation of neutron pickup. On the left of the vertical black lines the data are obtained with incomplete magnetic rigidity coverage.

points are shown in black. The vertical dashed (green) lines indicate the onset of neutron pickup, while the solid (black) lines mark the limits of the experimental completeness, constrained by incomplete magnetic rigidity coverage. As the figure demonstrates, several neutron-rich isotopes were produced.

In Fig. 1, we compare the experimental results (black points) with calculations from both the DIT and CoMD models. The DIT results are shown in blue lines and the CoMD in red lines. Dotted lines correspond to primary fragments, dashed lines to total calculations for the cold fragments, and full lines to calculations filtered for the experimental angular acceptance ($\Delta\theta = 2.2°$–$5.8°$) and magnetic rigidity coverage of the experiment. Overall, the DIT calculations reproduce the measured cross sections reasonably well and perform slightly better than the CoMD predictions.

Fig. 2 illustrates the CoMD results obtained with the different options of the symmetry potential. Experimental data are again shown by black points, while the standard CoMD calculation ($V_{\text{sym}}(\rho) \propto \rho$, where ρ is the density) is represented by red lines. The dashed lines indicate total cold fragments, and full lines represent the results filtered for the angular acceptance and magnetic rigidity coverage
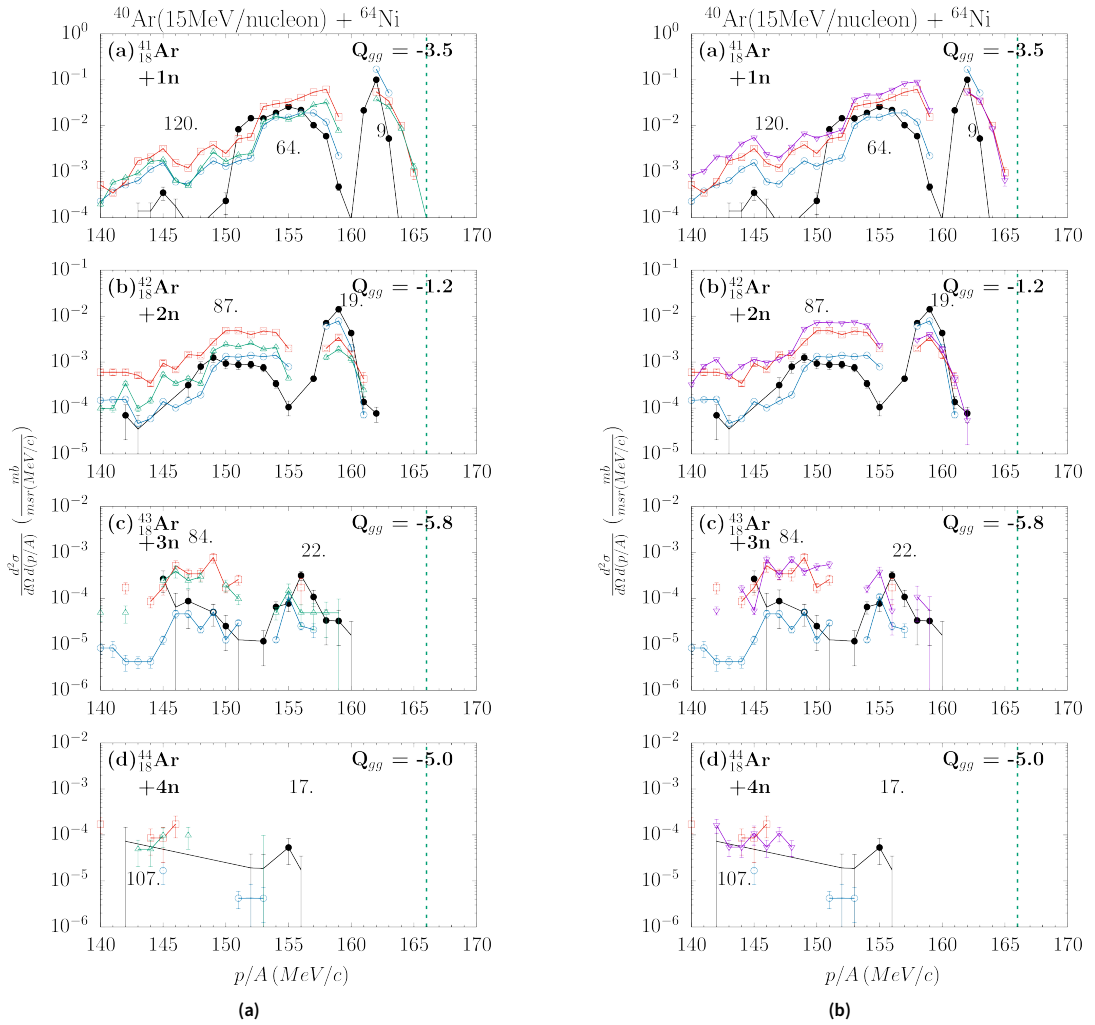
Figure 3. Momentum per nucleon distributions of projectile-like fragments for neutron pick-up channels. Black points: experimental data. Blue circles: DIT calculation. Red squares: CoMD calculation. The vertical dashed (green) lines indicate the velocity of the beam. (a): (a)–(d): Green triangles: CoMD calculation with stiff symmetry potential. (b): (a)–(d): Purple inverse triangles: CoMD calculation with soft symmetry potential.

Figure 4. Momentum per nucleon distributions of projectile-like fragments for proton removal channels. Black points: experimental data. Blue circles: DIT calculation. Red squares: CoMD calculation. The vertical dashed (green) lines indicate the velocity of the beam. (a): (a)–(d): Green triangles: CoMD calculation with stiff symmetry potential. (b): (a)–(d): Purple inverse triangles: CoMD calculation with soft symmetry potential.
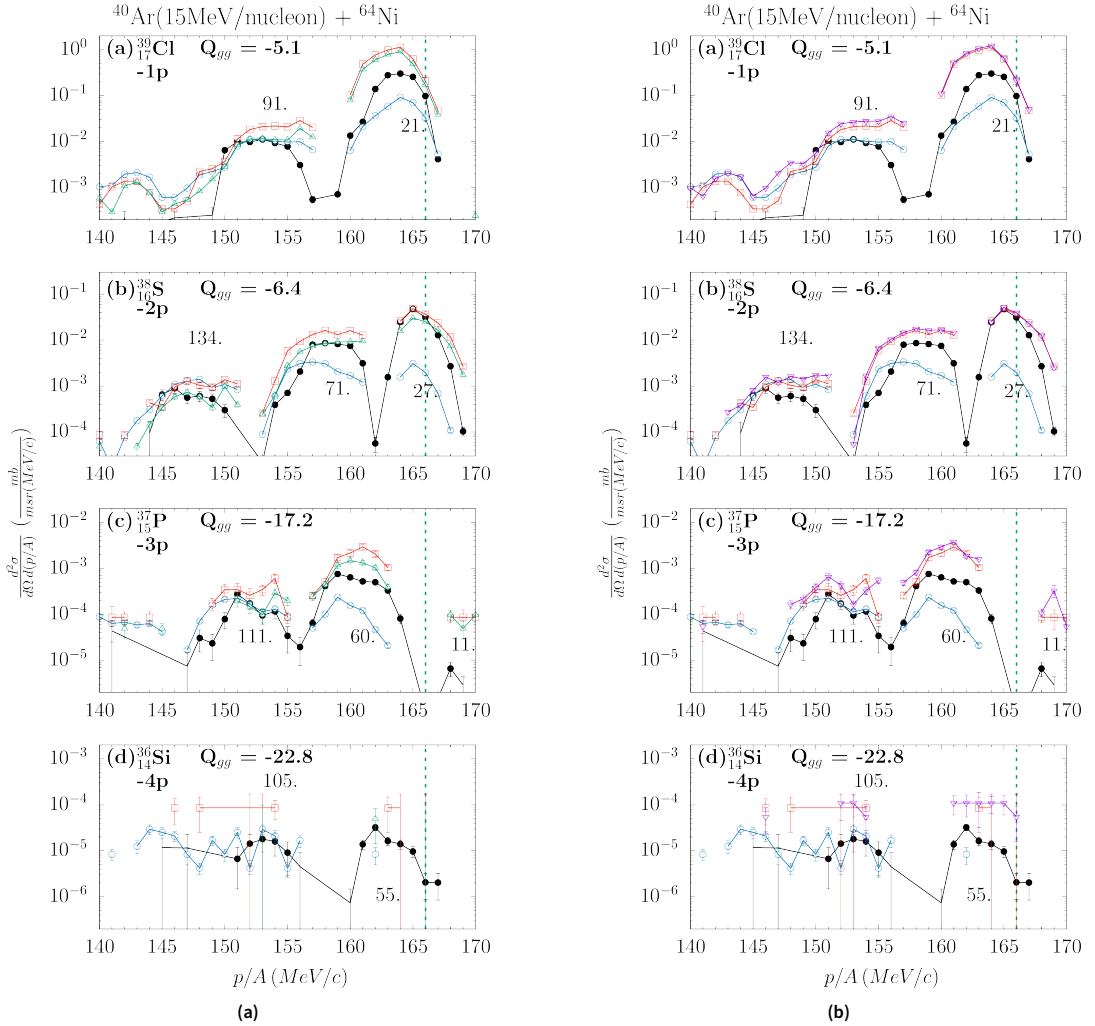
Figure 5. Momentum per nucleon distributions of projectile-like fragments for charge exchange channels. Black points: experimental data. Blue circles: DIT calculation. Red squares: CoMD calculation. The vertical dashed (green) lines indicate the velocity of the beam. (a): (a)–(d): Green triangles: CoMD calculation with stiff symmetry potential. (b): (a)–(d): Purple inverse triangles: CoMD calculation with soft symmetry potential.
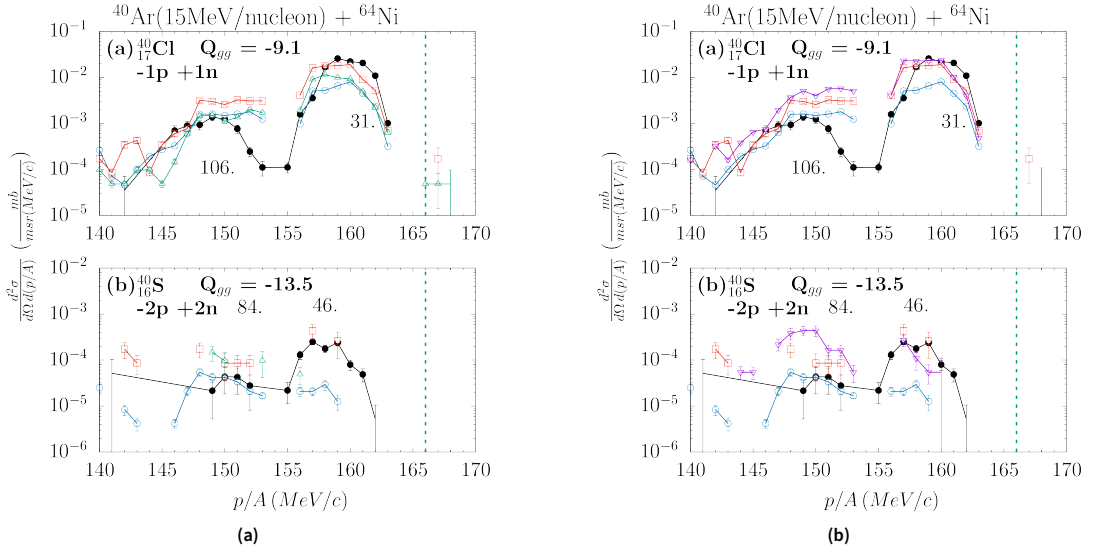
of the experiment. The CoMD calculation with a stiff symmetry potential ($V_{\text{sym}}(\rho) \propto \rho^2$) is shown in green, while that with a soft symmetry potential ($V_{\text{sym}}(\rho) \propto \sqrt{\rho}$) appears in purple.

Figs. 3, 4 and 5 present the momentum per nucleon (p/A) distributions for several reaction channels. These distributions are valuable for understanding the mechanisms responsible for fragment formation. The observed p/A reflects the degree of energy dissipation occurring in the projectile–target binary interaction. Two main regions can be distinguished: a quasi-elastic region at higher p/A values, corresponding to more direct processes, and a deep-inelastic region at lower p/A values, associated with extensive multinucleon transfers. Each row of panels corresponds to different reaction channels.

In Figs. 3a, 4a and 5a, we compare experimental data with the standard DIT and CoMD calculations, including the CoMD with a stiff symmetry potential; Figs. 3b, 4b and 5b show the corresponding results for the soft potential. Black points denote experimental data, blue circles indicate DIT results, red squares represent the CoMD standard calculation, green triangles correspond to the stiff symmetry potential, and purple inverted triangles to the soft potential. The vertical dashed (green) line marks the beam velocity. The numbers near selected points indicate the total excitation energy of the quasiprojectile–quasitarget system, derived from binary kinematics, and the corresponding p/A values. Q_{gg} represents the ground-state to ground-state Q-value of the reaction channel.

The dips observed in the experimental distributions are mainly due to incomplete magnetic rigidity coverage. In Fig. 3, we observe neutron pick-up channels, from one to four neutrons picked up, in Fig. 4, we observe proton removal chanels, from one to four protons removed, and in Fig. 5, we show the single and double charge exchange channels. All these channels lead to neutron-rich products. We can observe that the calculations with DIT and CoMD are more or less in overall agreement with the data, except the quasielastic part that may indicate the presence of direct nucleon transfer or other processes. The CoMD calculation with the stiff symmetry potential provides a slightly improved reproduction of the p/A distributions, particularly in reaction channels such as +1n, +2n,

-1p, -3p.

5. Conclusion and Future Plans

In summary, we have presented a detailed analysis of mass distributions and momentum per nucleon distributions for ejectiles from the ^{40}Ar + ^{64}Ni reaction at 15 MeV/nucleon. The experimental data, obtained using the MARS separator at the Cyclotron Institute of Texas A&M University in previous work of our group, were compared with calculations based on the DIT and CoMD dynamical models, followed by statistical de-excitation with GEMINI.

This study focused on channels producing neutron-rich products, up to four neutron pickup, up to four proton removal and single and double charge-exchange products. The theoretical results were filtered to account for the experimental angular acceptance and magnetic rigidity range, yielding good overall agreement with the data. A preliminary study of the symmetry potential has been performed. Within the CoMD model, stiff and soft options of the symmetry potential were explored, showing reasonable consistency with experimental trends. Ongoing analysis aims to further elucidate the effects of the symmetry potential parametrizations within CoMD, along with other parameters of the effective interaction implemented in the model.

In closing, we envision that future experiments employing other projectile–target systems will help extend this systematics and enhance our understanding of reaction mechanisms in the Fermi energy regime.

References

[1]   T. Mijatović. "Multinucleon transfer reactions: a mini-review of recent advances". In: *Front. Phys.* 10 (2022), p. 965198. DOI: 10.3389/fphy.2022.965198.

[2]   G. A. Souliotis, M. Veselsky, S. Galanopoulos, M. Jandel, Z. Kohley, L. W. May, D. V. Shetty, B. C. Stein, and S. J. Yennello. "Approaching neutron-rich nuclei toward the r-process path in peripheral heavy-ion collisions at 15 MeV/nucleon". In: *Phys. Rev. C* 84 (2011), p. 064607. DOI: 10.1103/PhysRevC.84.064607.

[3]   L. Corradi, G. Pollarolo, and S. Szilner. "Multinucleon transfer processes in heavy-ion reactions". In: *J. Phys. G: Nucl. Part. Phys.* 36 (2009), p. 113101. DOI: 10.1088/0954-3899/36/11/113101.

[4]   L. Corradi et al. "Multinucleon transfer reactions: Present status and perspectives". In: *Nucl. Instrum. Methods B* 317 (2013), pp. 743–751. DOI: 10.1016/j.nimb.2013.04.093.

[5]   A. Papageorgiou, G. A. Souliotis, K. Tshoo, S. C. Jeong, B. H. Kang, Y. K. Kwon, M. Veselsky, S. J. Yennello, and A. Bonasera. "Neutron-rich rare isotope production with stable and radioactive beams in the mass range A = 40–60 at beam energy around 15 MeV/nucleon". In: *J. Phys. G: Nucl. Part. Phys.* 45 (2018), p. 095105. DOI: 10.1088/1361-6471/aad7df.

[6]   K. Palli, G. A. Souliotis, T. Depastas, I. Dimitropoulos, O. Fasoula, S. Koulouris, M. Veselsky, S. J. Yennello, and A. Bonasera. "Microscopic dynamical description of multinucleon transfer in ^{40}Ar induced peripheral collisions at 15 MeV/nucleon". In: *EPJ Web Conf.* 252 (2021), p. 07002. DOI: 10.1051/epjconf/202125207002.

[7]   L. Tassan-Got and C. Stephan. "Deep inelastic transfers: a way to dissipate energy and angular momentum for reactions in the Fermi energy domain". In: *Nucl. Phys. A* 524 (1991), pp. 121–140. DOI: 10.1016/0375-9474(91)90019-3.

[8]   M. Papa, T. Maruyama, and A. Bonasera. "Constrained molecular dynamics approach to fermionic systems". In: *Phys. Rev. C* 64 (2001), p. 024612. DOI: 10.1103/PhysRevC.64.024612.

[9]   R. J. Charity et al. "Systematics of complex fragment emission in niobium-induced reactions". In: *Nucl. Phys. A* 483 (1988), pp. 371–405. DOI: 10.1016/0375-9474(88)90542-8.

[10] G. A. Souliotis, M. Veselsky, G. Chubarian, L. Trache, A. Keksis, E. Martin, D. V. Shetty, and S. J. Yennello. "Enhanced production of neutron-rich rare isotopes in peripheral collisions at Fermi energies". In: *Phys. Rev. Lett.* 91 (2003), p. 022701. DOI: 10.1103/PhysRevLett.91.022701.

[11] G. A. Souliotis, M. Veselsky, G. Chubarian, L. Trache, A. Keksis, E. Martin, A. Ruangma, E. Winchester, and S. J. Yennello. "Enhanced production of neutron-rich rare isotopes in the reaction of 25 MeV/nucleon ^{86}Kr on ^{64}Ni". In: *Phys. Lett. B* 543 (2002), pp. 163–172. DOI: 10.1016/S0370-2693(02)02459-0.

[12] O. Fasoula, G. A. Souliotis, S. Koulouris, K. Palli, M. Veselsky, S. J. Yennello, and A. Bonasera. "Momentum distribution studies of projectile fragments from peripheral collisions below the Fermi energy". In: *HNPS Adv. Nucl. Phys.* 29 (2023), pp. 38–44. DOI: 10.12681/hnpsanp.5089.

[13] S. Koulouris et al. "Multinucleon transfer channels from ^{70}Zn (15 MeV/nucleon) + ^{64}Ni collisions". In: *Phys. Rev. C* 108 (2023), p. 044612. DOI: 10.1103/PhysRevC.108.044612.

[14] R. E. Tribble, R. H. Burch, and C. A. Gagliardi. "MARS: A momentum achromat recoil spectrometer". In: *Nucl. Instrum. Methods Phys. Res. A* 285 (1989), pp. 441–446. DOI: 10.1016/0168-9002(89)90215-5.

[15] J. Klimo, M. Veselsky, G. A. Souliotis, and A. Bonasera. "Simulation of fusion and quasi-fission in nuclear reactions leading to the production of superheavy elements using the constrained molecular dynamics model". In: *Nucl. Phys. A* 992 (2019), p. 121640. DOI: 10.1016/j.nuclphysa.2019.121640.

[16] G. A. Souliotis, P. N. Fountas, M. Veselsky, S. Galanopoulos, Z. Kohley, A. McIntosh, S. J. Yennello, and A. Bonasera. "Isoscaling of heavy projectile residues and N/Z equilibration in peripheral heavy-ion collisions below the Fermi energy". In: *Phys. Rev. C* 90 (2014), p. 064612. DOI: 10.1103/PhysRevC.90.064612.